# Design of a Low-Capacitance Planar Transformer for a 4 kW/500 kHz DAB Converter

Pierre Demumieux, Oriol Avino-Salvado, Cyril Buttay, Christian Martin, Fabien Sixdenier, Charles Joubert, Jean Sylvio Ngoua Teu Magambo, Thomas Löher

# Design of a Low-Capacitance Planar Transformer for a 4 kW/500 kHz DAB Converter

Pierre Demumieux[1], Oriol Avino-Salvado[1], Cyril Buttay[1], Christian Martin[1], Fabien Sixdenier[1], Charles Joubert[1], Jean Sylvio Ngoua Teu Magambo[2], Thomas Löher [3]

[1] Univ Lyon, Université Claude Bernard Lyon 1, INSA-Lyon, CNRS, Ampère, F-69622, Villeurbanne, France
[2] Electrical & Electronics Division, Safran Tech - Safran Paris Saclay
[3] Fraunhöfer Institute for Reliability and Microintegration IZM, Technische Universität Berlin

***Abstract*—Increasing electrification in transport sectors, from automotive to aerospace, highlights the need for low size and high power density components. The recent advent of planar technology theoretically allows to reduce considerably the size of the magnetic components. This article focuses on the design of a high frequency planar transformer intended to be used in a 4 kW 500 kHz DAB converter. In particular, the inter-winding capacitances are assessed, as they have a strong influence on the behaviour of the DAB, and in some extreme cases may impede operation entirely. Analytical and finite element models are used to evaluate the stray elements of the transformer (resistance of the conductors, inter-winding capacitance and leakage inductance), and the resulting circuit model is compared with experimental measurements. This work focuses on influences of design parameters on the transformer stray elements.**

***Index Terms*—DAB, Planar Transformer, Stray Elements.**

## I. Introduction

The Dual Active Bridge (DAB) topology provides bidirectional dc–dc conversion using two inverters interconnected by an isolation transformer. Thanks to recent improvements in power devices (in particular the development of GaN transistors), the switching frequency of the inverters can be increased, which theoretically allows for a reduction in the size of the transformer according to the sizing relation of the area product (1).

$$A_e \cdot A_w = \frac{P_{max}}{kf \cdot k_B \cdot B_{peak} \cdot f \cdot J} \tag{1}$$

Thus, the core area $A_e$ and the winding area $A_w$ depend on the maximum power through the transformer $P_{max}$, the peak magnetic flux density in the core $B_{peak}$, the switching frequency $f$, the current density $J$, the waveform coefficient $k_f$ and the filling coefficient of the winding area $k_B$.

The DAB topology is particularly suited to low size thanks to the component count with respect to the power level of the converter. In addition, a design based on wide band gap and high frequency components allows to increase the power density of the converter.

The planar technology, which uses Printed Circuit Boards (PCBs) for the windings and low-profile magnetic cores, is attractive for the transformer. In particular, from the manufacturing to the thermal and EMC points of view, the planar technology offers better results than other high frequencies technologies such as Litz wire.

TABLE I: State of art of high power DC/DC Converter with planar transformer

| Year | Power [W] | Frequency [kHz] | Reference |
|---|---|---|---|
| LLC converter | | | |
| 2014 | 1000 | 1000 | [1] |
| 2016 | 3000 | 2500 | [2] |
| 2016 | 1200 | 300 | [3] |
| 2017 | 6600 | 500 | [4] |
| 2018 | 1000 | 1000 | [5] |
| Phase Shift Bridge converter | | | |
| 2014 | 3000 | 500 | [6] |
| Triple Active Bridge converter | | | |
| 2017 | 4500 | 70 to 150 | [7] |

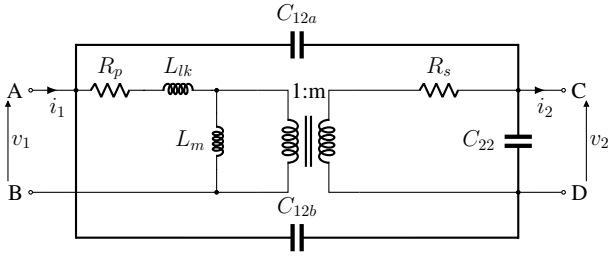


Fig. 1: Transformer modelling with 3 stray capacitances.

Tab. I highlights some recent publications regarding high frequency converters based on planar transformers

While they have many advantages, planar transformers geometries tend to have high stray capacitances that can seriously affect the global converter performances, so they must be designed with care.

Previous studies such as [8] have identified some analytical methods to predict stray capacitances values in the design process. Some papers have used the resulting high frequency transformer models to design and optimize dc–-dc isolated converters [3], [7]. Fig. 1 shows a classical inductive transformer model with the addition of three capacitances in parallel of each independent voltage [9].

As presented in Tab. I, the literature mainly focuses on the design of planar transformers for LLC topologies [4], [5]. For resonant topologies, the results show that the stray

TABLE II: Specifications of the converter

| Power [ W ] | Frequency [ kHz ] | Input Voltage [ V ] | Output Voltage [ V ] |
|---|---|---|---|
| 4000 | 500 | 100 | 300 |

TABLE III: Model parameters requirements

| Parameters | Lower limits | Upper limits | Sizing conditions |
|---|---|---|---|
| $L_{lk}$ | 250 nH | 450 nH | Max. RMS current and max. output power |
| $C_{12}$ | smallest as possible | 1 nF | Soft switching range (see Discussion section) |

capacitances in the transformer have no negative impact on the converter nor on modulations at high power and high frequency. In the DAB topology, the stray capacitances of the transformer add up to those of the switches and consequently have an effect on the operation of the converter.

In section II, the specifications of the converter will be detailed, presenting the limitations to take in account in the design. The methodology includes the design of the transformer and emphases the assessment of the circuit model. In section III, the circuit model is implemented in a Spice simulation of the converter and is confronted to the measurements on a mock-up version of the transformer.

This article gives some keys to define acceptable values for the stray capacitances in the transformer, in agreement with the range of soft switching in the converter. Further details are given in sections IV and V according to an analytical method confirmed by Spice simulation results.

The Spice model is used to understand the phenomena taking place in the converter and to analyze the impact of the stray capacitances in a DAB structure. An analytical model is proposed to determine the soft-switching operating range for given stray capacitances and leakage inductance of the transformer. This model is then used during the design of a planar transformer to find the optimal layout which meets our requirements.

## II. Context

The specifications of the converter are given in Tab. II. The consequences of these specifications on the model of the transformer from Fig. 1 are defined and presented in Tab. III and discussed below.

A transformer design cannot be built according to defined electrical parameters without considering some tolerance and that depending on many reasons (e.g. non-linear magnetic material, gap between magnetic core and PCB, PCB manufacturing tolerance). However, here, the method has been to define the limitations and consider them in an adjusted design.

The inductive parameters (e.g. magnetizing and leakage inductance) are easily estimated from the transfer function of the converter [10]. The magnetizing inductance, which has no impact on the energy transfer, needs to be set as high as possible to minimize the magnetizing current. The value of the leakage inductance is more constrained because it limits the operating and the soft switching ranges of the converter. If a too low value can be corrected by an additional inductance connected in series with the transformer, for high frequency applications, the most critical is the upper limit. Indeed, the maximum of the power transfer depends on the inductance value (2).

$$L_{series,max} = \frac{V_{in} \cdot \frac{V_{out}}{m}}{8 \cdot P_{max} \cdot f} \tag{2}$$

$L_{series,max}$ is the series inductance in the converter including the leakage inductance in the transformer but also the stray inductance in the active bridges.

Thereafter, from the range of operability for each parameter, a layout for the windings need to be defined. An interleaving of the windings is often necessary to optimize the losses and the thermal management of the design. Thus, the choice of the winding geometries becomes a trade-off between the resistance $R$, the inductance $L$ and the capacitance $C$.

TABLE IV: Parameters of the two transformer designs.

| | Transform. #1 | Transform. #2 |
|---|---|---|
| Magnetic core size | E64/10/50+PLT | 4x E80/38/20 |
| Winding area size (Width × High) | $23.8 \times 5.1$ | $19.7 \times 56.4$ |
| Primary turns — Transformer ratio | 2 — 3 | 2 — 3 |

## III. Methodology

### A. Designs overview

To demonstrate the effect of the windings geometries on the resulting transformer parameters, two configurations are presented in this paper, with for each a distinct core geometry. The first design is very flat, with a printed circuit board made as thin as possible. The second design is much taller and presents the possibility to adjust the legs height, allowing to study different geometries. The characteristics of both transformers are summarized in Table IV. Interleaved windings have been fostered, in both cases, to minimize losses and leakage inductances, as shown in the next sections. The primary turns are constituted by layers in parallel to limit the current density inside the primary winding.

The first transformer (#1) has been designed in order to minimize the leakage inductance and limit the transformer losses (windings and core) without taking into account the inter-winding capacitance constraint. The second one (#2) has been designed as a trade-off between the transformer losses, the leakage inductance and the inter-winding capacitance.

### B. Analytical evaluation of R, L and C in the transformer model

The methods used to evaluate the parasitic elements of a transformer are summarized here:

- The copper losses do not only depend on the DC resistance of the windings, but also on the effects of the frequency on the conductors such as eddy currents and proximity effects. That is why the concept of AC resistance $R_{ac}$ (3) is used to calculate the winding losses $P_{loss}$ (4) .

$$R_{ac,n} = F_{r,n} \cdot R_{dc} = F_{r,n} \cdot \rho \cdot \frac{N \cdot l}{S} \tag{3}$$

$$P_{loss} = \sum_{i=1}^{n} (R_{ac,n} \cdot I_{rms,n}^2) \tag{4}$$

The number of turns $N$, the length of a turn $l$ and the cross section $S$ of one conductor set the DC resistance of the windings. The frequency effects (e.g. Skin and Proximity effects) depend on the geometry and the positioning of windings. These effects are calculated accurately by means of "Eddy currents" solver using Finite Element Modellers (FEM) such as Ansys Maxwell®. Analytical calculations are also possible using Dowell-like models [11], [12], but they are generally less accurate.

- The leakage inductance [11] is related to the magnetic energy outside of the magnetic core (5), where the magnetic field is calculated (6) using the Ampere's law.

$$E_{Llk} = \frac{1}{2} \int_{vol} B \cdot H \cdot dV = \frac{1}{2} \cdot L_{lk} \cdot I_{peak}^2 \tag{5}$$

$$\sum_{n=1}^{N} I_{peak} = \oint H \cdot dl \tag{6}$$

FEM magnetostatic simulations allow to compute the self $L_{xx}$ and mutual $M_{xx}$ inductances of the windings. From these results, the coupling coefficient (7) and the leakage inductance (8) are calculated.

$$k = \frac{M_{12}}{\sqrt{L_{11} \cdot L_{22}}} \tag{7}$$

$$L_{lk} = (1 - k^2) \cdot L_{11} \tag{8}$$

- The stray capacitances depend on winding configuration of the transformer. In the case of interleaved primary/secondary windings, with large copper conductors, this stray capacitance can be estimated using the classical plane capacitor equation:

$$C_{stray} = N_{face} \cdot \varepsilon_0 \cdot \varepsilon_r \cdot \frac{S_{face}}{e_{FR4}} \tag{9}$$

The geometric parameters impacting the capacitance are the number of sufaces facing each other $N_{face}$ or their surface area $S_{face}$ and the insulation spacing $e_{FR4}$. Electrostatic FEM simulations are also performed to confirm $C_{stray}$ values as well as to evaluate the stray capacitance of each winding.

As an example, a two turns transformer (see 2a) shows the oposition between inductances and capacitances evolution versus the insulation thickness for a transformer composed of only one turn for both primary and secondary windings. The result is given in Fig. 2b and while the inter-winding capacitance exhibits a hyperbola, the leakage inductance increases almost linearly.

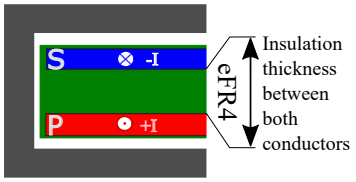


(a) Cross section of a transformer, with the primary (red) and secondary (blue) conductors separated by FR4 material (Dielectric constant: $\varepsilon_r \approx 5$) (green).

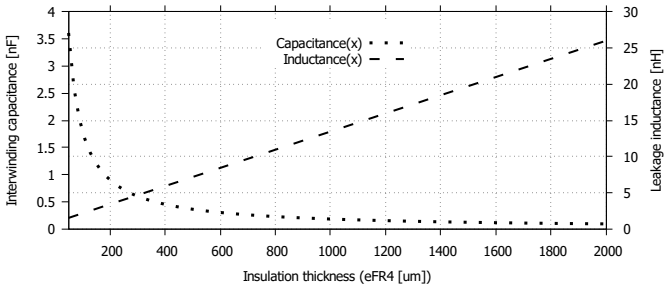


(b) Variation in inter-winding capacitance and leakage inductance as a function of the thickness of the insulating layer.

Fig. 2: Analytical results on two layer transformer

## IV. Results

### A. Winding design

Fig. 3 presents some layouts from a non-interleaved solution to a fullly-interleaved solution. For each layout, a first leading key element was to minimize the number of turns to reduce the total length of the windings without increasing the flux density inside the core too much. In addition, some layers were connected in parallel to realize one turn and reduce the current density in the layers. The three different designs presented in Fig. 3 all have the same number of turns. Only the interleaving changes between primary and secondary layers.

One key parameter of all solutions presented in Fig. 3 is the dielectric thickness. Indeed, this parameter is of prime importance for voltage insulation and then several material (preimpregnated glass fiber sheets, or prepregs) thicknesses were developed in the electronic industry to fulfill this constraint.

The main challenges are:

- Assessing the leakage inductance from the magnetomotive force diagrams: one insulating layer from another do not have the same influence on the leakage inductance according to the magnetic field $H(A/m)$. It should also be noted than layouts 3b and 3c share the same magnetomotive force maximum. In comparison from the others, the non-interleaved solutions presents a higher magnetomotive force than the other, which impacts badly the resistance and the leakage inductance of the transformer. That is why, the non-interleaved solutions is excluded from the workable solutions.
- Considering the capacitances between facing surfaces, we dissociated the insulating layers $Pr1$ experiencing mag-

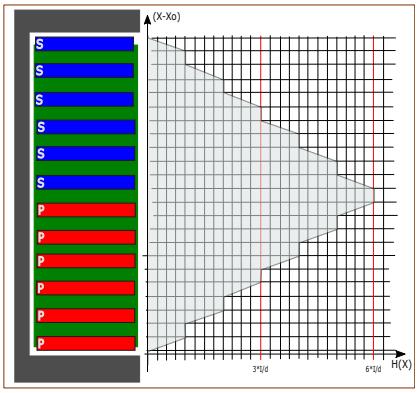


(a) Non-interleaved solution (...P-P-P-S-S-S...).

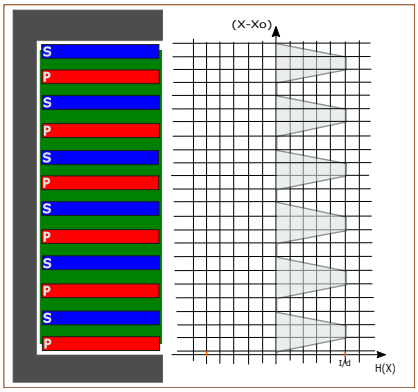


(b) Fully-interleaved solution (P-S-P-S-P-S...).

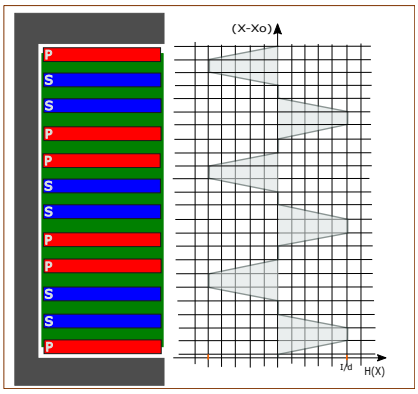


(c) Alternative interleaving solution (P-S-S-P-P-S...).

Fig. 3: Transformer layout studied by analytical and simulation tools with the corresponding magnetomotive force diagram.

netic field and the insulating layers $Pr2$ without magnetic field. The first group of layers ($Pr1$) influences both the leakage inductance and the capacitance according to each layer thickness $h_{Pr1}$, whereas the second one $Pr2$, with a thickness $h_{Pr2}$, affects only the capacitance. Fig. 4a and 4b show the inter-winding capacitance isovalues in the $h_{Pr2}$ versus $h_{Pr1}$ plane for the designs presented in Fig. 3b and 3c respectively. It can be seen that for a given value of inter-winding capacitance, this value depends on both $h_{Pr1}$ and $h_{Pr2}$ for a fully-interleaved solution

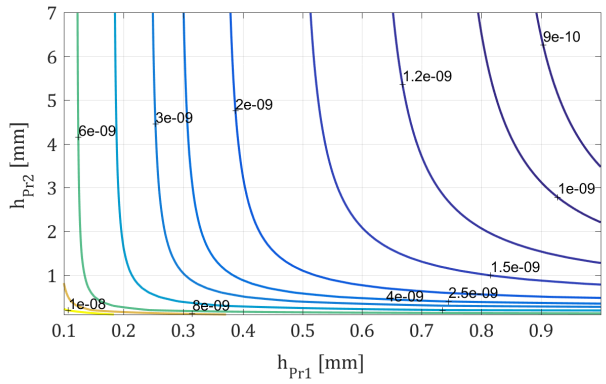


(a) Inter-winding capacitance – fully-interleaved (Fig. 3b).

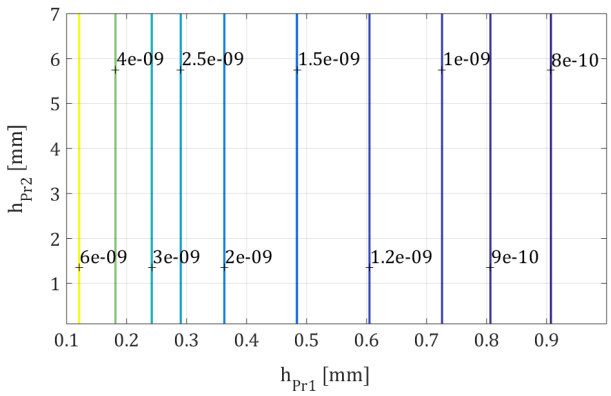


(b) Inter-winding capacitance – alternative interleaving (Fig. 3c).

Fig. 4: Parametric assessment of the inter-winding capacitance according to the insulation thickness $h_{Pr1}$ and $h_{Pr2}$ (Transformer with 4x E80/38/20 - For one turn: Length: 150 mm; Width: 17mm)

TABLE V: Inter-winding capacitance, leakage inductance of both transformer designs, as measured with an Impedance analyzer.

| | Transformer #1 | Transformer #2 |
|---|---|---|
| Inter-winding capacitance | 16 nF | 400 pF |
| Leakage inductance | 80 nH | 150nH |

(Fig. 4a) whereas it only depends only on $h_{Pr1}$ for the alternative interleaving solution (Fig. 4b). In conclusion, it should be pointed out that the layout 3c allows to have less inter-winding capacitance than 3b for the same insulation thicknesses. Nevertheless, the layout 3c leads to increase a little bit the intra-winding capacitance, but the difference from the layout 3b is not significant. For this reason, the result is not shown.

### *B. Experimentation and measurement*

The results of parameters identification from measurements on both transformer, designed with full-interleaved winding,prototypes are summarized in Tab. IV. The main difference

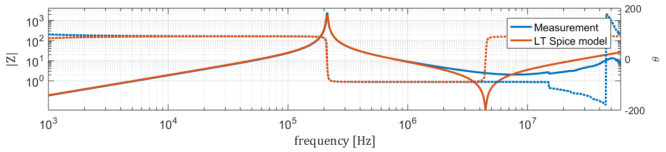


(a) On the primary winding - Secondary winding in open circuit.

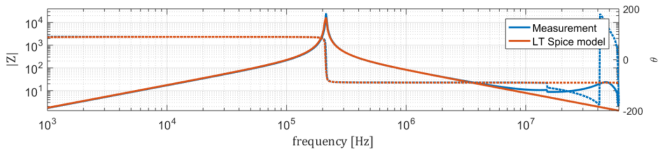


(b) On the secondary winding - Primary winding in open circuit.

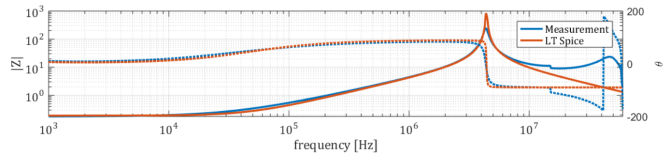


(c) On the secondary winding - Primary winding in short-circuited.

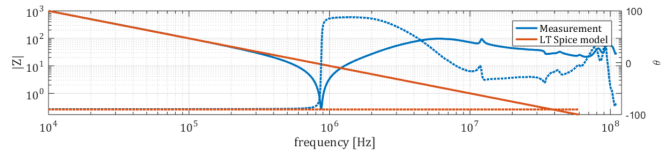


(d) Between primary and secondary winding - all windings are short-circuited.

Fig. 5: Impedance (module and phase) as a function of frequency, measured and simulated

is the inter-winding capacitance, which is 40 times smaller for design #2 than for design #1, with only a twofold corresponding increase in leakage inductance.

### C. Modelling and correlation with measurements

A circuit model of the transformer (Fig. 1) is required for the simulation of the DAB converter. LT Spice (Linear Technology) has been selected as the circuit simulator because of its flexibility and its compatibility with available GaN transistor models. The first step is to check the model accuracy in comparison with a functional prototype (transformer #1).

A comparison between simulations (LT Spice AC analysis) and measurements (using a Keysight E4990A Impedance Analyzer) is presented in Fig. 5 for different configurations (open/short circuit, primary/secondary measurements). From these results, the circuit model shows a satisfying match with the measurements. Its identification is based on the same protocol as developed in [9], [13].

Tab. VI gives the analytical expression of resonnant points for all the measurements.

## V. Discussion

### A. Impact of the transformer parasitic capacitances on a DAB

As frequency increases, the impedance of the capacitances drops while that of the inductances increases. There is a change in behaviour (from inductive to capacitive) of the transformer. The capacitances take a predominant place in its high frequency behaviour beyond the resonant point. The risk is, obviously, to lose the magnetic coupling between primary and secondary.

Another problem, specific to the DAB topology is the shrinkage of the soft-switching operating range of the converter. This phenomenon has been highlighted by LT Spice transient simulation of the full system. Here, the DAB converter is controlled by phase shift modulation [14] between the primary and the secondary full bridge inverters. The switches are modellized by GaN component (GS 66516T) models from GaN System [15]. Four transistors are implemented in parallel for each $Q$ switch. Fig. 6 presents the circuit of the DAB converter and Tab. VII presents some key parameters of the simulation.

TABLE VI: Identification of the transformer parameters.

| Tests | Resonant frequencies $f_r$ | Dominant feature |
|---|---|---|
| Open-circuit Primary side | $\frac{1}{2\,\pi\cdot\sqrt{(L_{m1}\cdot(C_{12a}+C_{12b}))}}$ | Magnetizing inductance $L_{m1}$ |
| Open-circuit Secondary side | $\frac{1}{2\,\pi\cdot\sqrt{(L_{m2}\cdot m^2\cdot(C_{12a}+C_{12b}))}}$ | Magnetizing inductance $L_{m2}$ |
| Short-circuit Secondary side | $\frac{1}{2\,\pi\cdot\sqrt{(L_{lk2}\cdot(C_{12a}+C_{12b}))}}$ | Leakage inductance $L_{lk2}$ |

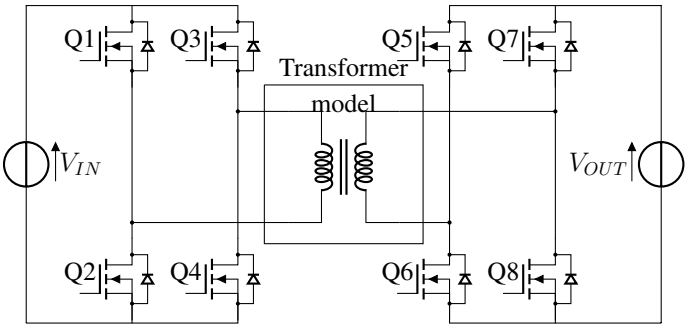


Fig. 6: DAB converter

TABLE VII: Input data for LT Spice simulation

| Part | Parameters/ components | Value/model |
|---|---|---|
| DC input | Voltage source | 100 V |
| Output | DC load | 4kW / 300V |
| Switches | 4 transistor in // | GS66516T L2V2 [15] |
| Control | Phase shift between primary and secondary | 42 degrees |
| Switching frequency | - | 500 kHz |
| Transformer seen from primary side | Transformer ratio<br>Leakage inductance<br>Magnetizing inductance<br>Intra-winding capacitance | 1:3<br>450 nH<br>31 $\mu$H<br>250 pF |

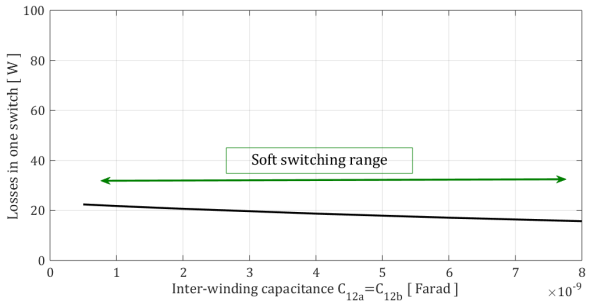


(a) Losses in one switch - Primary side

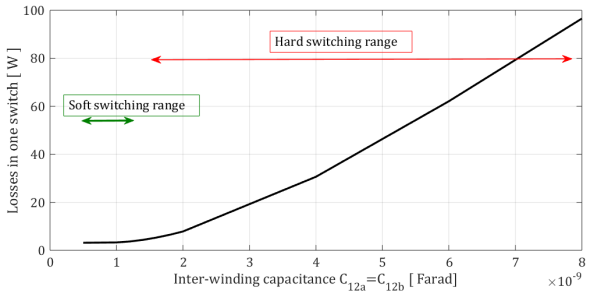


(b) Losses in one switch - Secondary side

Fig. 7: Results of parametric LT Spice simulation depending on the stray capacitances value of the transformer

First the global measured inter-winding capacitance has to be split into two equal parts ($C_{12a} = C_{12b} = C_{inter-winding}/2$, see Fig. 1). Then step-parametric simulations are performed for $C_{inter-winding}$ ranging from 250 pF (transformer #2) to 8 nF (i.e. transformer #1) out and losses in one switch are analyzed.

The results are given in Fig. 7. For the primary side 7a, the stray capacitances have low influence on the losses, but, on the secondary side 7b, they are multiplied by 30 between the best case (low capacitance value) and worst case (high capacitance value). The behaviour is not linear and can be resumed by two asymptotic curves. The first one is close to an horizontal curve and depending only on the conduction losses, whereas the second one is strongly increasing.

### *B. Analytical interpretation of the physical behaviour*

This phenomenon depends on the switching conditions for a DAB topology. For a good understanding of this behaviour and the influence of the transformer stray capacitances, the soft-switching range of a DAB structure is assessed analytically.

The operating of a DAB converter with single phase shift control has been detailed in many publications [10], [14], [16]. As emphasized in these articles, with the single phase shift modulation, DAB converters have some limitations of operation, and soft switching ranges depend on the input and output voltages as well as the value of current at switching times for the primary and secondary bridges. This first condition is presented in the literature [10] such as in Fig. 8.

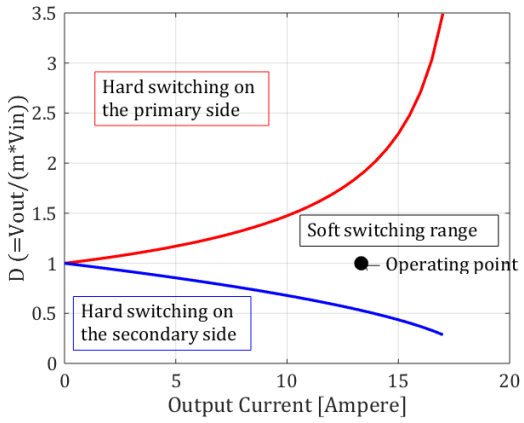


Fig. 8: Hard switching conditions

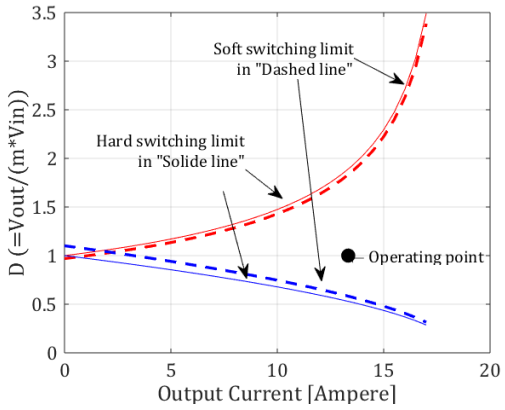


Fig. 9: Soft switching conditions without the transformer capacitances

In addition, the ZVS (i.e. Zero Voltage Switching) relies on the discharge of the output capacitances of the transistors using the leakage inductance of the transformer. To ensure this function, the energy stored in the serial inductance $E_{Llk}$ has to be superior or at least equal to the energy stored in the output capacitances $E_{C_{DS}}$ (eq.10).

$$E_{Llk} \geq E_{C_{DS}}$$

$$\frac{1}{2} \cdot L_{lk} \cdot (I_{peak})^2 \geq \frac{1}{2} \cdot C_{DS} \cdot (U_{Drain\ Source})^2 \qquad (10)$$

More accurately, with the addition of this constraint, the soft switching and hard switching limits are no longer superimposed. The converter can be in another position between soft switching and hard switching. Taking into account the output capacitances of the four transistors in parallel ($4 \cdot Coss$), the soft switching limitations are depicted in Fig.9.

However, in Fig. 9, null capacitances in the transformer has been assumed implicitly. A more realistic (albeit simplified, as it only considers one side of the converter) model of the whole converter with stray capacitances of the transformer is

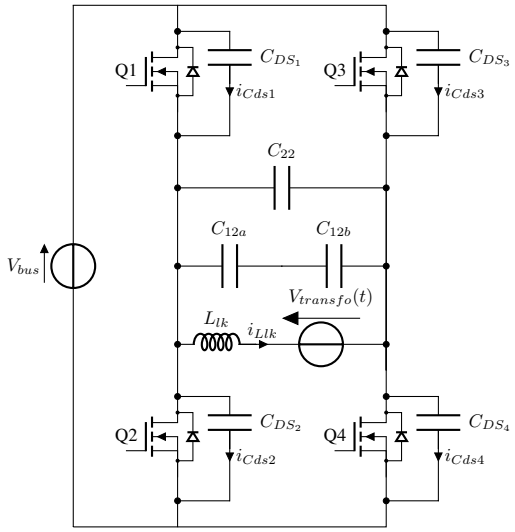


Fig. 10: Equivalent circuit diagram of a full bridge with the transformer model

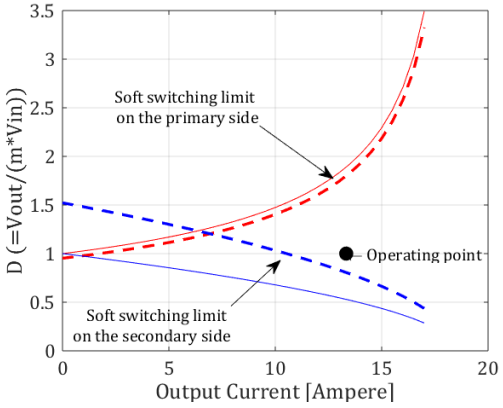


Fig. 11: Soft switching conditions with the transformer capacitances ($C_{12a} = C_{12b} = 1\ nF; C_{22} = 250\ pF$ )

shown in Fig. 10. The schematic is relevant for both sides of the converter. Thus, $V_{bus}$ can be the DC voltage in the input or in the converter output and $V_{transfo}(t)$ is the winding electromotive force.

From this model, (10) can be completed as (11).

$$E_{Llk} \geq E_{C_{DS}}$$
$$\frac{1}{2} \cdot L_{lk} \cdot (I_{peak})^2 \geq \frac{1}{2} \cdot (C_{DS} + \frac{C_{12}}{2} + C_{22}) \cdot (U_{DS})^2 \quad (11)$$

Then the realistic soft switching limits are given in Fig. 11

From these results it can be seen that the higher are the interwinding capacitances, the smaller the soft switching range is. The soft switching limit on the primary side is not very different from the previous case, whereas on the secondary side, the soft switching limits are highly affected by the interwinding capacitances, so much that the operating point is now close to this limit. This is due to the boost behaviour of the converter (e.g high voltage and low current on the secondary side; low voltage and high current on the primary side).

## VI. Conclusion

- In this article, a design method has been proposed for a planar transformer with a special focus on DAB applications. This study emphases the effects of stray capacitances on the DAB.
- FEM simulations and analytical models were compared with measurements on 2 transformer prototypes to analyze losses, inductances and capacitances. Both methods produced equivalent results. It has been shown that modifying the design parameters can have a dramatic influence on the inter-winding capacitance, while maintaining the leakage inductance at an acceptable level.
- The proposed analytical method allowed to determine the effects of stray capacitances of a high power/high frequency planar transformer on the soft switching conditions of DAB converter.It has been constated that stray capacitances can significatively reduce soft-switching region, for high frequencies applications. Thus, the research of "low stray capacitances" winding geometries become necessary in the design process for planar transformer.

## Acknowledgment

The GaNOMIC project receives funding from the European Union's Horizon 2020 research and innovation programme under Grant Agreement No 730038.

Authors would like thank their partners and colleagues from TU Berlin for the prototype manufacturing.

## References

[1] D. Huang, S. Ji, and F. C. Lee, "Llc resonant converter with matrix transformer," in *2014 IEEE Applied Power Electronics Conference and Exposition - APEC 2014*, pp. 1118–1125, March 2014.

[2] C. Armbruster, A. Hensel, A. H. Wienhausen, and D. Kranzer, "Application of gan power transistors in a 2.5 mhz llc dc/dc converter for compact and efficient power conversion," in *2016 18th European Conference on Power Electronics and Applications (EPE'16 ECCE Europe)*, pp. 1–7, Sept 2016.

[3] M. A. Saket, N. Shafiei, and M. Ordonez, "Planar transformer winding technique for reduced capacitance in llc power converters," in *2016 IEEE Energy Conversion Congress and Exposition (ECCE)*, pp. 1–6, Sept 2016.

[4] B. Li, Q. Li, and F. C. Lee, "A novel pcb winding transformer with controllable leakage integration for a 6.6kw 500khz high efficiency high density bi-directional on-board charger," in *2017 IEEE Applied Power Electronics Conference and Exposition (APEC)*, pp. 2917–2924, March 2017.

[5] R. Chen and S. Yu, "A high-efficiency high-power-density 1mhz llc converter with gan devices and integrated transformer," in *2018 IEEE Applied Power Electronics Conference and Exposition (APEC)*, pp. 791–796, March 2018.

[6] M. Pahlevaninezhad, D. Hamza, and P. K. Jain, "An improved layout strategy for common-mode emi suppression applicable to high-frequency planar transformers in high-power dc/dc converters used for electric vehicles," *IEEE Transactions on Power Electronics*, vol. 29, pp. 1211–1228, March 2014.

[7] J. S. N. T. Magambo, R. Bakri, X. Margueron, P. L. Moigne, A. Mahe, S. Guguen, and T. Bensalah, "Planar magnetic components in more electric aircraft: Review of technology and key parameters for dc dc power electronic converter," *IEEE Transactions on Transportation Electrification*, vol. 3, pp. 831–842, Dec 2017.

[8] J. Biela and J. W. Kolar, "Using transformer parasitics for resonant converters - a review of the calculation of the stray capacitance of transformers," in *Fourtieth IAS Annual Meeting. Conference Record of the 2005 Industry Applications Conference, 2005.*, vol. 3, pp. 1868–1875 Vol. 3, Oct 2005.

[9] A. Besri, H. Chazal, and J. P. Keradec, "Capacitive behavior of hf power transformers: Global approach to draw robust equivalent circuits and experimental characterization," in *2009 IEEE Instrumentation and Measurement Technology Conference*, pp. 1262–1267, May 2009.

[10] A. R. Alonso, J. Sebastian, D. G. Lamar, M. M. Hernando, and A. Vazquez, "An overall study of a dual active bridge for bidirectional dc/dc conversion," in *2010 IEEE Energy Conversion Congress and Exposition*, pp. 1129–1135, Sept 2010.

[11] P. L. Dowell, "Effects of eddy currents in transformer windings," *Electrical Engineers, Proceedings of the Institution of*, vol. 113, pp. 1387–1394, August 1966.

[12] J. A. Ferreira, "Improved analytical modeling of conductive losses in magnetic components," *IEEE Transactions on Power Electronics*, vol. 9, pp. 127–131, Jan 1994.

[13] A. Schellmanns, *Circuits equivalents pour transformateurs multienroulements : Application a la CEM conduite d'un convertisseur*. Theses, Institut National Polytechnique de Grenoble - INPG, July 1999.

[14] K. George, "Design and control of a bidirectional dual active bridge dc-dc converter to interface solar, battery storage, and grid-tied inverters," Master's thesis, UARK, 2015.

[15] GaNSystems, "Gansystems website." https://gansystems.com/gan-transistors/gs66516t/.

[16] F. Krismer, S. Round, and J. W. Kolar, "Performance optimization of a high current dual active bridge with a wide operating voltage range," in *2006 37th IEEE Power Electronics Specialists Conference*, pp. 1–7, June 2006.